Since January 2020 Elsevier has created a COVID-19 resource centre with free information in English and Mandarin on the novel coronavirus COVID-19. The COVID-19 resource centre is hosted on Elsevier Connect, the company's public news and information website.

Elsevier hereby grants permission to make all its COVID-19-related research that is available on the COVID-19 resource centre - including this research content - immediately available in PubMed Central and other publicly funded repositories, such as the WHO COVID database with rights for unrestricted research re-use and analyses in any form or by any means with acknowledgement of the original source. These permissions are granted for free by Elsevier for as long as the COVID-19 resource centre remains active.

Journal of Immunological Methods 489 (2021) 112937

Contents lists available at ScienceDirect

Journal of Immunological Methods

journal homepage: www.elsevier.com/locate/jim

Research paper

Comparative analyses of SARS-CoV-2 binding (IgG, IgM, IgA) and neutralizing antibodies from human serum samples

Livia Mazzini [a], Donata Martinuzzi [b], Inesa Hyseni [b], Linda Benincasa [b], Eleonora Molesti [b,*], Elisa Casa [b], Giulia Lapini [a], Pietro Piu [a], Claudia Maria Trombetta [c], Serena Marchi [c], Ilaria Razzano [b], Alessandro Manenti [a,b], Emanuele Montomoli [a,b,c]

[a] VisMederi S.r.l., Siena, Italy
[b] VisMederi Research S.r.l., Siena, Italy
[c] Department of Molecular and Developmental Medicine, University of Siena, Siena, Italy

ARTICLE INFO

Keywords:
ELISA
SARS-CoV-2
Human samples
Micro-neutralization
Receptor-binding domain

ABSTRACT

A newly identified coronavirus, named SARS-CoV-2, emerged in December 2019 in Hubei Province, China, and quickly spread throughout the world; so far, it has caused more than 49.7 million cases of disease and 1,2 million deaths. The diagnosis of SARS-CoV-2 infection is currently based on the detection of viral RNA in nasopharyngeal swabs by means of molecular-based assays, such as real-time RT-PCR. Furthermore, serological assays detecting different classes of antibodies constitute an excellent surveillance strategy for gathering information on the humoral immune response to infection and the spread of the virus through the population. In addition, it can contribute to evaluate the immunogenicity of novel future vaccines and medicines for the treatment and prevention of COVID-19 disease.

The aim of this study was to determine SARS-CoV-2-specific antibodies in human serum samples by means of different commercial and in-house ELISA kits, in order to evaluate and compare their results first with one another and then with those yielded by functional assays using wild-type virus. It is important to identify the level of SARS-CoV-2-specific IgM, IgG and IgA antibodies in order to predict human population immunity, possible cross-reactivity with other coronaviruses and to identify potentially infectious subjects.

In addition, in a small sub-group of samples, a subtyping IgG ELISA has been performed. Our findings showed a notable statistical correlation between the neutralization titers and the IgG, IgM and IgA ELISA responses against the receptor-binding domain of the spike protein. Thus confirming that antibodies against this portion of the virus spike protein are highly neutralizing and that the ELISA Receptor-Binding Domain-based assay can be used as a valid surrogate for the neutralization assay in laboratories that do not have biosecurity level-3 facilities.

1. Introduction

Coronaviruses (CoVs) are enveloped, positive single-stranded RNA viruses belonging to the *Coronaviridae* subfamily. The Coronavirus subfamily comprises 4 Genera: Alpha-coronavirus which contains the human coronavirus (HCoV)-229E and HCoV-NL63; Beta-coronavirus which includes HCoV-OC43, Severe Acute Respiratory Syndrome human coronavirus (SARS-CoV-1), Middle Eastern respiratory syndrome coronavirus (MERS-CoV) and the newly emerged Severe Acute Respiratory Syndrome Coronavirus 2 (SARS-CoV-2).

Several members of this family, such as HCoV OC43, NL63 and 229E, cause mild common colds every year in the human population (Corman et al., 2019). Three highly pathogenic novel CoVs have appeared in the last 18 years; SARS-CoV-1 virus emerged in November 2002 in Guangdong province, causing more than 8,000 confirmed cases and 774 deaths (de Wit et al., 2016; Gorbalenya et al., 2020), MERS-CoV virus was discovered in June 2012 (Zaki et al., 2012) causing 2494 laboratory confirmed cases including 858 associated deaths, and SARS-CoV-2 virus emerged in Wuhan, Hubei province, China, in December 2019; this last was declared a pandemic on March 11th 2020 by the World Health Organization (WHO). The global impact of the SARS-CoV-2 outbreak, with over 49,7 million COVID-19 cases and 1,2 million deaths reported to WHO (as of 10th November 2020) (WHO, n.d.-a), is unprecedented.

Several data have confirmed that the infection initially arose from

* Corresponding author at: VisMederi Research S.r.l., 53100 Siena, Italy.
E-mail address: eleonora.molesti@vismederiresearch.com (E. Molesti).

https://doi.org/10.1016/j.jim.2020.112937
Received 24 September 2020; Received in revised form 17 November 2020; Accepted 23 November 2020
Available online 28 November 2020
0022-1759/© 2020 The Authors. Published by Elsevier B.V. This is an open access article under the CC BY license (http://creativecommons.org/licenses/by/4.0/).

contact with animals in the Wuhan seafood market. Subsequently, human-to-human transmission occurred, leading to a very high rate of laboratory-confirmed infections in China (Chan et al., 2020; WHO, 2020). Precise diagnosis of Coronavirus disease (COVID-19) is essential in order to promptly identify infected individuals, to limit the spread of the virus and to allow those who have been infected to be treated in the early phases of the infection. To date, real-time polymerase chain reaction (RT-PCR) is the most widely employed method of diagnosing COVID-19. However, rapid, large-scale testing has been prevented by the high volume of demand and the shortage of the materials needed for mucosal sampling (Zou et al., 2020). Standardized serological assays able to measure antibody responses may help to overcome these issues and may support a significant number of relevant applications. Indeed, serological assays are the basis on which to establish the rate of infection (severe, mild and asymptomatic) in a given area, to calculate the percentage of the population susceptible to the virus and to determine the fatality rate of the disease. It has been demonstrated in a non-human primate model (Bao et al., 2020) that, once the antibody response has been established, re-infection and, consequently, viral shedding, is unlikely. Furthermore, serological assays can help to identify subjects with strong antibody responses, who could serve as donors for the generation of monoclonal antibody therapeutics (Andreano et al., 2020).

The spike glycoprotein (S-protein), a large transmembrane homotrimer of approximately 140 kDa, has a pivotal role in viral pathogenesis, mediating binding to target cells through the interaction between its receptor-binding domain (RBD) (Wrapp et al., 2020) and the human angiotensin converting enzyme 2 (ACE2) receptor. The S-protein has been found to be highly immunogenic, and the RBD is possibly considered the main target in the effort to elicit potent neutralizing antibodies (Tay et al., 2020; Berry et al., 2010). Two subunits constitutes the S-protein: S1, which mediates attachment, and the S2, which mediates membrane fusion. The CoV S-protein is a class I fusion protein, and protease cleavage is required for activation of the fusion process (Ou et al., 2016).

To date, the complexity of the systemic immunoglobulin G (IgG) together with IgG subclasses and IgM and IgA, in terms of responses against SARS-CoV-2, have not been elucidated yet. Moreover, data comparing the differences between these responses and the neutralizing responses detected by functional assays such as Micro-Neutralization test (MN), are still not well defined.

Undoubtedly, it is well recognized that the IgG levels have a crucial role for protection from viral disease (Murin et al., 2019). In humans, the four IgG subclasses (IgG1, IgG2, IgG3, IgG4) differ in function (Schroeder and Cavacini, 2010) and IgG1 and IgG3 play a key role in many fundamental immunological functions, including virus neutralization, opsonization and complement fixation (Frasca et al., 2013). Therefore, we conducted a comparative study for two purposes: the first aim was to investigate the sensitivity and specificity, in terms of detection, of different ELISA kits compared with MN results; the second objective was to investigate the difference relatively to the spike-RBD-specific IgG, IgM and IgA antibody responses in human serum samples.

2. Materials and methods

2.1. Serum samples

In March/April 2020, 181 human serum samples were collected by the laboratory of Molecular Epidemiology of the University of Siena, Italy. The samples were anonymously collected in compliance with Italian ethics law.

Three human serum samples from confirmed cases of COVID-19 were kindly provided by Prof. Valentina Bollati from the University of Milan, Italy. Human IgG1 anti-SARS-CoV-2 Spike (S1) antibody CR3022 (Native Antigen,21 Drydock Avenue, 7th Floor Boston, MA 02210, USA), Human IgM anti-SARS-CoV-2 Spike (S1) Antibody CR3022 (Native Antigen, Oxford, UK) and anti-Spike RBD (SARS-CoV-2/COVID 19) human monoclonal antibody (eEnzyme, Gaithersburg, USA) were used as positive controls in ELISA. Human serum minus (IgA/IgM/IgG) (Cod. S5393, Sigma, St. Louis, USA) was also used as a negative control in MN assay and ELISA.

Three human serum samples containing heterologous neutralizing antibodies, provided by NIBSC (WHO 1st International Standard for Pertussis antiserum (lot. 06/140); WHO 2nd International Standard for antibody to influenza H1N1pdm virus (lot. 10/202); WHO 1st International Standard for Diphtheria Antitoxin (lot: 10/262)), plus a panel of commercial human serum samples ($n = 26$, provided by BioIVT company (West Sussex, United Kingdom), with confirmed non SARS-CoV-2 virus cross reactivity (positive towards different HCoVs), were used to verify the specificity of the ELISA test.

2.2. Cell culture

Vero E6 cells, acquired from the American Type Culture Collection (ATCC - CRL 1586), were cultured in Dulbecco's Modified Eagle's Medium (DMEM) - High Glucose (Euroclone, Pero, Italy) supplemented with 2 mM L-Glutamine (Lonza, Milan, Italy), 100 units/mL penicillin-streptomycin mixture (Lonza, Milan, Italy) and 10% of Fetal Bovine Serum (FBS), at 37 °C, in a 5% CO_2 humidified incubator.

VERO E6 cells were seeded in a 96-well plate using D-MEM high glucose 2% FBS at a density of 1.5×10^6 cells per well, in order to obtain a 70–80% sub-confluent cell monolayer after 24 h.

2.3. SARS-CoV-2 purified antigen, live virus and titration

Five different purified recombinant S proteins (S1 and RBD domain) were tested for their ability to detect specific human antibodies: S1-SARS-CoV-2 (HEK293) Cod. REC31806-500, (Native Antigen, Oxford, UK); S1-SARS-CoV-2 (HEK293) Cod. SCV2-S1-150P (eEnzyme, Gaithersburg, MD, USA); S1-SARS-CoV-2 (HEK293) Cod. S1N-C52H3 (ACROBiosystems, Newark, DE, USA); Spike RBD-SARS-CoV-2 (Baculovirus-Insect cells) Cod. 40592-V08B and (HEK293) Cod. 40592-V08H (Sino Biological, Beijing, China).

SARS CoV-2 - strain *2019-nCov/Italy-INMI1* – wild-type virus was purchased from the European Virus Archive Global (EVAg, Spallanzani Institute, Via Portuense, 292, 00148-00153, Rome). The virus was titrated in Biosecurity Level 3 laboratories (BSL) in serial 1-log dilutions to obtain a 50% tissue culture infective dose ($TCID_{50}$) on 96-well culture plates of VERO E6 cells. The plates have been observed daily for the presence of cytopathic effect (CPE) by means of an inverted optical microscope for a total of 4 days. The end-point titers were calculated according to the Spearman-Karber formula (Kundi, 1999).

2.4. Micro-neutralization assay

The MN assay was performed as previously reported by Manenti et al. (Manenti et al., 2020). Briefly, 2-fold serial dilutions of heat-inactivated serum samples were mixed with an equal volume of viral solution containing 100 $TCID_{50}$ of SARS-CoV-2. The serum-virus mixture was incubated for 1 h at 37 °C in a humidified atmosphere with 5% CO_2. After incubation, 100 μL of the mixture at each dilution was passed to a 96-well cell plate containing a 70–80% confluent VERO E6 monolayer. The plates were incubated for 3 days at 37 °C in a humidified atmosphere with 5% CO_2. After the incubation time, each well was inspected by means of an inverted optical microscope to evaluate the percentage of CPE. The highest serum dilution that protected more than 50% of cells from CPE was taken as the neutralization titer.

2.5. Commercial Enzyme-Linked Immunosorbent Assay (ELISA)

Specific anti-SARS-CoV-2 IgG antibodies were detected by means of the Euroimmun commercial ELISA kit.

Euroimmun-ELISA plates were coated with recombinant structural

protein (S1 domain) of SARS-CoV-2. The assay provides semi-quantitative results by calculating the ratio of the optical density (OD) of the serum sample over the OD of the calibrator. According to the manufacturer's instructions, positive samples have a ratio $\geq$ 1.1, borderline samples a ratio between 0.8 and 1.1 and negative samples a ratio $<$ 0.8.

2.5.1. In-House S1 and RBD Enzyme-Linked Immunosorbent Assay (ELISA) IgG, IgM and IgA

ELISA plates were coated with 1 μg/mL of purified recombinant Spike S1 Protein (aa 18–676) (eEnzyme, Gaithersburg, MD, USA) or with 1 μg/mL Spike-RBD (Arg319-Phe541) (Sino Biological, China), both expressed and purified from HEK 293 cells. After overnight incubation at +4 °C, coated plates were washed three times with 300 μL/well of ELISA washing solution containing Tris Buffered Saline (TBS)-0.05% Tween 20, then blocked for 1 h at 37 °C with a solution of TBS containing 5% of Non-Fat Dry Milk (NFDM; Euroclone, Pero, Italy). Serum samples were heat-inactivated at 56 °C for 1 h in order to reduce the risk of the presence of live virus in the sample. Subsequently, 3-fold serial dilutions, starting from 1:100 in TBS-0.05% Tween 20 5% NFDM, were performed up to 1:2700. Plates were washed three times, as previously; then 100 μL of each serial dilution was added to the coated plates by means of a multichannel pipette and incubated for 1 h at 37 °C. Next, after the washing step, 100 μL/well of Goat anti-Human IgG-Fc Horse Radish Peroxidase (HRP)-conjugated antibody or IgM (μ-chain) and IgA (α- chain) diluted 1:100,000 or 1:100,000 and 1:75,000, respectively, (Bethyl Laboratories, Montgomery USA) were added. Plates were incubated at 37 °C for 30 min. Following incubation, plates were washed and 100 μL/well of 3,3′,5,5′-Tetramethylbenzidine (TMB) substrate (Bethyl Laboratories, Montgomery, USA) was added and incubated in the dark at room temperature for 20 min. The reaction was stopped by adding 100 μL of ELISA stop solution (Bethyl Laboratories, Montgomery, USA) and read within 20 min at 450 nm. To evaluate the OD a SpectraMax ELISA plate (Medical Device) reader was used.

A cut-off value was defined as 3 times the average of OD values from blank wells (background: no addition of analyte). Samples with the ODs under the cut off value at the first 1:100 dilution were assigned as negative, samples where the ODs at 1:100 dilution were above the cut-off value were assigned as positive. Borderline samples were defined where one replicate was under the cut-off and the other was above.

2.5.2. In-house RBD Enzyme-Linked Immunosorbent Assay (ELISA) IgG1, IgG2, IgG3 and IgG4

An indirect ELISA was performed in order to determine the RBD-specific IgG1, IgG2, IgG3 and IgG4 antibody concentration in serum samples (Manenti et al., 2017). 96-well plates were coated with 1 μg/mL of purified Spike-RBD (Sino Biologicals). Serum samples were diluted from 1:50 to 1:400. Mouse anti-human IgG1, IgG2, IgG3 and IgG4 Fc-HRP (Southern Biotech, USA) secondary antibodies were used at 1:8000 dilution. The cut-off values were established as reported above (paragraph 1.5.1).

2.6. Generation of depleted-IgA serum

ELISA plates were coated with 10 μg/mL of high affinity purified goat anti-human IgA antibodies (Bethyl Laboratories) than blocked for 1 h at 37 °C. 10 μL of each heat inactivated serum sample (positive for MN and IgA ELISA) were then seeded in an ELISA coated plate and incubated for 2 h at 37 °C. After the incubation time the serum samples were harvested and stored at +4 °C until the MN assay.

2.7. Statistical analysis

Spearman's rank correlation analysis enabled us to determine whether, and to what extent, the MN assay was associated with the ELISAs. A classification analysis gave further insight into the relationship between the MN and the in-house ELISAs. We defined the MN as the target variable and recoded its results by assigning the label "0" to values of 5, and the label "1" otherwise. We implemented an elastic net (EN) to classify the Micro-neutralization titers (MNT). The EN is a rather sophisticated generalized linear model (GLM), which addresses the issues caused by multi-collinearity among predictors. We set the binomial family for the GLM after dichotomizing the variable MNT; therefore, we followed a logistic-like model approach in the implementation of the EN. The EN produces a selection of the variables based on a convex penalty function, which is a combination of the ridge regression and the LASSO (Least Absolute Shrinkage and Selection Operator) penalties, say l1 and l2 respectively, controlled by the hyper-parameter alpha = l2/(l1 + l2). The hyper-parameter, lambda, by contrast, regulates the level of penalization in the model (Zou and Hastie, 2005). To improve the generalization capability of the EN, we trained the model over a randomly selected subset of data (121/181) and verified its robustness over an independent subset of the residual data (60/181), which did not enter the model during the training stage. The cross-validation technique prevented the occurrence of over-fitting problems in the estimates. On the base of the values of the predictors of the test set, X, and their estimated EN coefficients, b, we built a score function, S, as follows:

$$S(X,b) = e^{X \cdot b}$$

The probability of a positive MNT assignment for the predicted results was then expressed as:

$$P(MNT = \text{Positive}) = \frac{S(X,b)}{(1 + S(X,b))}$$

We calculated the performance of the EN in terms of sensitivity, i.e., the percentage of positive MNT correctly predicted, and specificity, i.e., the percentage of negative MNT correctly predicted, and represented their related Receiver Operating Characteristic (ROC) curve. The optimal combination of sensitivity and specificity enabled us to detect the cut-off in the score function; test samples were classified as positive if their score was above this cut-off value and as negative if the score was below it, with the minimum error probability.

3. Results

3.1. Set-up and standardization of in-house ELISAs

Several purified recombinant S-proteins (S1 and RBD domain) were tested for their ability to detect specific human antibodies: S1-SARS-CoV-2 (HEK293) (from Native Antigen); S1-SARS-CoV-2 (HEK293) (from eEnzyme); S1-SARS-CoV-2 (HEK293) (from ACROBiosystems); Spike RBD-SARS-CoV-2 (Baculovirus-Insect cells) and (HEK293) (from Sino Biological). Each protein was evaluated using three coating concentrations (1, 2 and 3 μg/mL) and four different dilutions of the secondary HRP conjugate anti-human IgG, IgM and IgA antibodies. The optimal concentration chosen for antigen coating was 1 microgram/mL while the optimal dilution for the secondary HRP conjugate anti-human IgG, IgM was 1:100,000 and 1: 75,000 for anti-Human IgA. We also evaluated the impact of the incubation time of the HRP by incubating the plates for 1 h or 30 min, and concluded that the best and clearest signal was always seen after the shortest incubation. To set the assays, three human serum samples derived from convalescent donors, along with a pool of MN and ELISA (commercial Kit)-negative human serum samples, were used as positive and negative controls, respectively. As a test control, human IgG1 monoclonal antibody (mAb) anti-SARS-CoV-2 spike (S1) (CR3022 Native antigen), human IgM mAb anti-SARS-CoV-2 spike (S1) (CR3022 Absolute antibody) and human IgG1 anti-Spike RBD (SCV2-RBD eEnzyme) were used. Additionally, several human sera hyper-immune to various infectious diseases (influenza, diphtheria and pertussis) were used to assess the specificity of the assay in detecting

Table 1
Comparative table showing the results obtained when human sera were tested by different ELISA kits and by micro neutralization test (MN).

ID Sample	Elisa Euroimmun	MNT titer	ELISA_VM_IgG_S1	ELISA_VM_IgG_RBD	ELISA_VM_IgM_S1	ELISA_VM_IgM_RBD	ELISA_VM_IgA_RBD
From 1 to 8	Negative	5	Negative	Negative	Negative	Negative	Negative
9	Negative	5	Negative	Negative	Negative	Positive	Negative
10–11	Negative	5	Negative	Negative	Negative	Negative	Negative
12	Negative	5	Negative	Negative	Negative	Positive	Negative
13	Negative	5	Negative	Negative	Negative	Negative	Negative
14	Borderline	5	Negative	Negative	Negative	Negative	Negative
15	Negative	5	Negative	Negative	Negative	Negative	Negative
16	Negative	5	Negative	Negative	Positive	Negative	Negative
From 17 to 21	Negative	5	Negative	Negative	Negative	Negative	Negative
22	Borderline	5	Positive	Negative	Negative	Negative	Negative
From 23 to 31	Negative	5	Negative	Negative	Negative	Negative	Negative
32	Negative	5	Negative	Positive	Negative	Negative	Negative
From 33 to 36	Negative	5	Negative	Negative	Negative	Negative	Negative
37	Positive	5	Negative	Negative	Negative	Positive	Negative
38–39	Negative	5	Negative	Negative	Negative	Negative	Negative
40	Positive	5	Negative	Negative	Negative	Negative	Negative
41	Negative	5	Negative	Negative	Negative	Negative	Negative
42	Borderline	5	Negative	Negative	Negative	Negative	Negative
43	Positive	5	Positive	Positive	Negative	Negative	Negative
44–45	Negative	5	Negative	Negative	Negative	Negative	Negative
46	Positive	5	Positive	Negative	Negative	Negative	Negative
From 47 TO 49	Negative	5	Negative	Negative	Negative	Negative	Negative
50	Negative	5	Negative	Negative	Negative	Positive	Negative
51–52	Negative	5	Negative	Negative	Negative	Negative	Negative
53	Negative	5	Negative	Negative	Negative	Positive	Negative
From 54 to 60	Negative	5	Negative	Negative	Negative	Negative	Negative
61	Positive	5	Negative	Negative	Negative	Negative	Negative
62	Negative	5	Positive	Negative	Negative	Negative	Negative
63–64	Negative	5	Negative	Negative	Negative	Negative	Negative
65	Borderline	5	Negative	Negative	Negative	Negative	Negative
66–67	Negative	5	Negative	Negative	Negative	Negative	Negative
68	Positive	5	Positive	Negative	Negative	Positive	Negative
69	Positive	5	Positive	Negative	Negative	Negative	Negative
From 70 to 72	Negative	5	Negative	Negative	Negative	Negative	Negative
73	Borderline	5	Negative	Negative	Negative	Negative	Negative
From**74 to 76**	Negative	5	Negative	Negative	Negative	Negative	Negative
77	Positive	5	Positive	Negative	Negative	Negative	Negative
78	Borderline	5	Negative	Negative	Positive	Negative	Negative
79	Borderline	5	Negative	Negative	Negative	Negative	Negative
80	Positive	5	Negative	Negative	Negative	Negative	Negative
81	Borderline	5	Negative	Negative	Negative	Negative	Negative
From 82 to 91	Negative	5	Negative	Negative	Negative	Negative	Negative
92	Positive	5	Positive	Negative	Negative	Positive	Negative
93	Borderline	5	Positive	Negative	Positive	Negative	Negative
94–95	Negative	5	Negative	Negative	Negative	Negative	Negative
96	Negative	5	Negative	Negative	Negative	Positive	Negative
97–98	Negative	5	Negative	Negative	Negative	Negative	Negative
99	Positive	5	Positive	Negative	Negative	Negative	Negative
From 100 to 107	Negative	5	Negative	Negative	Negative	Negative	Negative
108	Negative	5	Negative	Negative	Negative	Positive	Positive
109	Negative	5	Negative	Negative	Positive	Negative	Negative
110	Negative	5	Negative	Negative	Positive	Positive	Negative
111	Negative	5	Negative	Negative	Positive	Positive	Negative
112	Negative	5	Negative	Negative	Negative	Negative	Negative
113	Positive	5	Positive	Positive	Positive	Positive	Negative
From 114 to 117	Negative	5	Negative	Negative	Negative	Negative	Negative
118	Negative	5	Negative	Negative	Positive	Negative	Negative
119–120	Negative	5	Negative	Negative	Negative	Negative	Negative
121	Positive	5	Positive	Negative	Positive	Negative	Negative
From 122 to 127	Negative	5	Negative	Negative	Negative	Negative	Negative
128	Positive	5	Positive	Positive	Negative	Negative	Positive
129	Negative	5	Negative	Negative	Negative	Negative	Negative
130	Negative	5	Negative	Negative	Negative	Positive	Negative
131–132	Negative	5	Negative	Negative	Negative	Negative	Negative
133	Positive	5	Positive	Negative	Negative	Negative	Negative
From 134 to 142	Negative	5	Negative	Negative	Negative	Negative	Negative
143	Negative	5	Negative	Negative	Negative	Positive	Negative
from 144 to 146	Negative	5	Negative	Negative	Negative	Negative	Negative
147	Negative	5	Negative	Negative	Positive	Positive	Negative
148	Negative	5	Negative	Negative	Negative	Negative	Negative
149	Negative	5	Negative	Negative	Negative	Positive	Negative
150	Positive	5	Positive	Positive	Negative	Negative	Negative
151	Negative	5	Negative	Negative	Negative	Negative	Negative

(*continued on next page*)

Table 1 (*continued*)

ID Sample	Elisa Euroimmun	MNT titer	ELISA_VM_IgG_S1	ELISA_VM_IgG_RBD	ELISA_VM_IgM_S1	ELISA_VM_IgM_RBD	ELISA_VM_IgA_RBD
152	Positive	5	Positive	Negative	Negative	Negative	Negative
153	Negative	5	Negative	Negative	Negative	Negative	Negative
154	Negative	10	Negative	Negative	Negative	Positive	Negative
155	Positive	1280	Positive	Positive	Positive	Positive	Positive
156	Negative	10	Negative	Positive	Negative	Negative	Negative
157	Negative	10	Negative	Negative	Positive	Negative	Negative
158	Positive	20	Positive	Positive	Negative	Positive	Positive
159	Negative	20	Negative	Positive	Negative	Positive	Positive
160	Negative	20	Negative	Negative	Negative	Negative	Positive
161	Negative	20	Negative	Negative	Positive	Negative	Negative
162	Negative	20	Negative	Positive	Positive	Positive	Positive
163	Positive	40	Positive	Positive	Positive	Positive	Positive
164	Negative	40	Negative	Positive	Negative	Positive	Negative
165	Negative	40	Negative	Positive	Negative	Positive	Positive
166	Negative	80	Negative	Positive	Negative	Positive	Positive
167	Borderline	80	Negative	Positive	Positive	Positive	Negative
168	Negative	80	Positive	Positive	Negative	Positive	Positive
169	Negative	80	Negative	Positive	Negative	Positive	Positive
170	Positive	80	Positive	Positive	Positive	Positive	Positive
171	Negative	160	Negative	Positive	Negative	Positive	Positive
172	Positive	160	Positive	Positive	Negative	Positive	Positive
173	Positive	160	Positive	Positive	Positive	Positive	Negative
174	Positive	320	Negative	Positive	Positive	Positive	Positive
175–176	Positive	640	Positive	Positive	Positive	Positive	Positive
177	Positive	640	Positive	Positive	Negative	Positive	Positive
178–179	Positive	640	Positive	Positive	Positive	Positive	Positive
180–181	Positive	1280	Positive	Positive	Positive	Positive	Positive

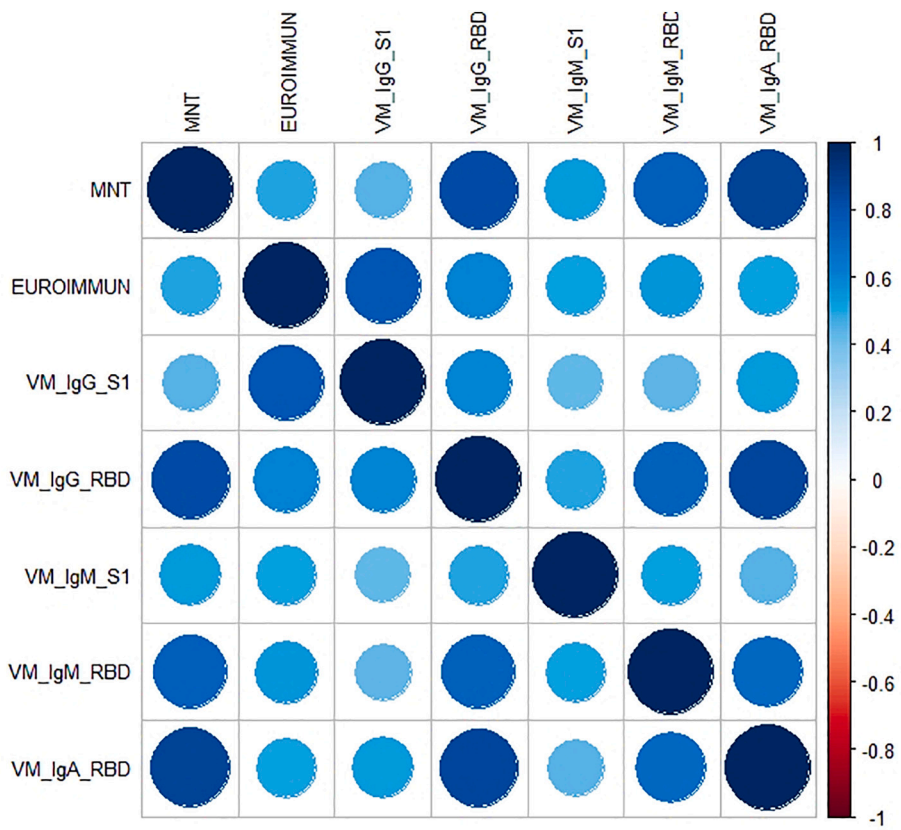

Fig. 1. The correlation plot associated to the measured coefficients of Spearman's rank correlation. The magnitude of the coefficient is represented by circles and a color gradient: the larger the area of the circle and the more intense the tone of the color, the greater the correlation. The direction of the correlation is indicated by the color scale: blue tones for positive correlations and red tones for negative correlations. (For interpretation of the references to color in this figure legend, the reader is referred to the web version of this article.)

only antibodies against SARS-CoV-2 S1 or the RBD protein. Alternative blocking/diluent solutions containing 1% Bovine Serum Albumin (BSA), 2.5% milk and 5% milk were tested. The specificity of the test increased significantly on using the 5% milk blocking solution in comparison with BSA, which occasionally yielded non-specific results and displayed a generally higher background. Finally, the two proteins that yielded the best results in terms of sensitivity and specificity were chosen as candidates for the tests: the purified S1-protein (HEK derived) from eEnzyme and the Purified RBD protein (HEK derived) from Sino Biological.

Table 2
Specificity of in House ELISA test for IgG and IgM responses against SARS-CoV-2 RBD.

Sample ID	ELISA In house RBD - IgG	ELISA In house RBD - IgM
368424 SR1 COVID-19 IgG/IgM	POS	POS
368424 SR1 COVID-19+ IgG/IgM	POS	POS
368424 SR1 COVID-19+ IgG/IgM	POS	POS
368424 SR1 COVID-19+ IgG/IgM	POS	POS
373,647-SR1 COVID-19+ IgG	POS	POS
373647-SR1 COVID-19+ IgG	POS	NEG
373647-SR1 COVID-19+ IgG	POS	NEG
373647-SR1 COVID-19+ IgG	POS	NEG
HMN406906 **229E**+	NEG	NEG
HMN406954 **OC43/229E**+	NEG	NEG
HMN406901 **OC43/229E**+	NEG	NEG
HMN406939 **229E**+	NEG	NEG
HMN406903 **HKU/OC43/229E**+	NEG	NEG
HMN406909 **HKU/OC43/229E**+	NEG	NEG
HMN406913 **HKU/OC43/229E**+	NEG	NEG
HMN406910 **HKU/OC43/229E/ NL63**+	NEG	NEG
HMN406927 **HKU/OC43/229E**+	NEG	NEG
HMN406944 **OC43/229E**+	NEG	NEG
HMN406945 **OC43/229E**+	NEG	NEG
HMN406919 **OC43/229E/ NL63**+	NEG	NEG
HMN406924 **229E/NL63**+	NEG	NEG
HMN406929 **HKU/OC43/229E**+	NEG	NEG
HMN406920 **HKU/OC43/229E/ NL63**+	NEG	NEG
HMN406922 **HKU/OC43/229E**+	NEG	NEG
HMN406933 **HKU/OC43/229E/ NL63**+	NEG	NEG
HMN406938 **HKU/OC43/229E**+	NEG	NEG

3.2. Correlation between ELISAs and Neutralization

Each serum sample was tested by means of *in-house* ELISA S1 and RBD-specific IgG, IgM and IgA (VM_IgG_S1, VM_IgG_RBD, VM_IgM_S1, VM_IgM_RBD, VM_IgA_RBD) and by means of the Euroimmun S1 Commercial ELISA kit, along with the functional MN assay (Table 1). The distribution of the micro-neutralization titers (MNTs) was strongly asymmetric, with most of the values (153/181) being equal to 5 (i.e. negative). The other values observed (from 10 to 1280 in a 2-fold dilution series) were uniformly distributed. Concerning the ELISA S1, we performed two different tests: one by means of a commercial (Euroimmun) kit and the other an in-house ELISA. According to Spearman's rank correlation coefficients and statistical significance (Tables 3 and 4), we registered the highest agreement between the ELISA VM_IgG_RBD and MNT, and between the VM_IgA_RBD and MNT, with coefficients of 0.83 and 0.85, respectively. The lowest correlations were found for ELISA Euroimmun vs MNT, and for VM_IgG_S1 vs MNT, with coefficients of 0.49 and 0.45, respectively. As can be seen from the correlation plot (Fig. 1), the IgA response was closely linked with a positive MN response. Moreover, on dissecting all the results for each serum sample (data not shown), we noted that, in those subjects in whom we registered a high neutralization titer, we always observed a positive IgA signal.

Interestingly, in 9 MNT-positive samples, we found a complete absence of S1 signal on using Euroimmun, VM_IgG_S1 and VM_IgM_S1 ELISA kits but, on the other hand, high and detectable IgG and IgM RBD-specific signals.

To confirm the analytical specificity of the in-house RBD of the in-house RBD-ELISA test, commercial human serum samples with confirmed non-SARS-COV-2 Coronavirus cross-reactivity (positives towards different HCoVs) were tested and the selectivity of this test to discriminate between IgG/IgM and IgG only responses in COVID-19 positive samples was evaluated. Among these samples 5 were confirmed positives for IgG and IgM, while 3 samples were confirmed IgG positives and IgM negatives. For all the remaining 18 samples, positives towards different HCoV strains, (from n.9 to n.26) no cross-reactivity was confirmed and these panel of sera were tested by In-house RBD ELISA (Table 2).

3.3. Classification analysis: elastic net

Over a training set of data, the optimal hyper-parameters estimated for the Elastic Net (EN) model were lambda = 0.0136 and alpha = 0.76, which minimized the error of cross-validation (=0.3809). The EN model selected three significant predictors of the MN results, namely VM-IgG-RBD, VM-IgM-RBD, and VM-IgA-RBD; the estimates of their coefficients were 0.0035, 0.0060 and 0.0013, respectively, while the intercept of the model was −2.9741. These results were entered into the score function, whereby we predicted the MNTs. From the ROC curve (Fig. 2A), we evaluated the performance of the predictions in terms of sensitivity and specificity. On balancing sensitivity and specificity, we obtained the optimal cut-off of 0.092, with sensitivity = 85.7% (95% CI = [42.1%–99.6%]) and specificity = 98.1% (95% CI = [89.9%–99.6%]) (Fig. 2B). Overall, these findings indicated that the in-house RBD-based ELISA methods were highly accurate and, particularly, presented the features of a highly specific diagnostic test when jointly considered.

The samples, which yielded a score below the identified cut-off, were classified as "negative", and the remaining samples as "positive". We then compared these predictions with the known results of the test-set (Fig. 2C).

Analysis of the error matrix indicated an overall Accuracy (ACC) of 96.7% (95% CI = [88.5%–99.6%]), and a No Information Rate (NIR) of 88.3% (95% CI = [77.4%–95.2%]). Since the ACC was significantly higher than the NIR ($p = 0.02$), we may claim that the model built with the In-house (VM) RBD-based ELISAs conveyed effective information. The extremely high value of the odds ratio (OR) = 312.0, (95% CI = [17.2–5657.7]) revealed the strong association between the MN results and the model predictions. Specifically, the positive predictions were 312 times more likely to occur in association with positive MNT than the negative predictions.

3.4. IgG subtyping of serum samples

We also evaluated the ELISA IgG subtyping response (IgG1, IgG2, IgG3, and IgG4) in a small subgroup (14) of MN-positive samples. ELISA plates were coated with RBD purified antigen. Our results, although derived from a small group of subjects, are in line with previous findings by Amanat and colleagues (Amanat et al., 2020). Strong reactivity for

Table 3
Spearman's rank correlation coefficients.

	MNT	EUROIMMUN	VM_IgG_S1	VM_IgG_RBD	VM_IgM_S1	VM_IgM_RBD	VM_IgA_RBD
MNT	1.00	0.49	0.45	0.83	0.52	0.73	0.85
EUROIMMUN	0.49	1.00	0.77	0.59	0.50	0.54	0.51
VM_IgG_S1	0.45	0.77	1.00	0.59	0.43	0.44	0.53
VM_IgG_RBD	0.83	0.59	0.59	1.00	0.49	0.73	0.84
VM_IgM_S1	0.52	0.50	0.43	0.49	1.00	0.50	0.45
VM_IgM_RBD	0.73	0.54	0.44	0.73	0.50	1.00	0.69
VM_IgA_RBD	0.85	0.51	0.53	0.84	0.45	0.69	1.00

Table 4
Statistical significance of Spearman's rank correlation coefficients.

	MNT	EUROIMMUN	VM_IgG_S1	VM_IgG_RBD	VM_IgM_S1	VM_IgM_RBD	VM_IgA_RBD
MNT	0.0E+00	3.8E-07	3.3E-10	8.1E-47	3.5E-14	1.5E-31	7.0E-53
EUROIMMUN	3.8E-07	0.0E+00	2.8E-20	1.9E-10	1.8E-07	1.5E-08	1.3E-07
VM_IgG_S1	3.3E-10	2.8E-20	0.0E+00	3.4E-18	2.1E-09	5.8E-10	2.1E-14
VM_IgG_RBD	8.1E-47	1.9E-10	3.4E-18	0.0E+00	1.5E-12	3.1E-31	2.5E-50
VM_IgM_S1	3.5E-14	1.8E-07	2.1E-09	1.5E-12	0.0E+00	5.5E-13	3.1E-10
VM_IgM_RBD	1.5E-31	1.5E-08	5.8E-10	3.1E-31	5.5E-13	0.0E+00	2.9E-27
VM_IgA_RBD	7.0E-53	1.3E-07	2.1E-14	2.5E-50	3.1E-10	2.9E-27	0.0E+00

Table 5
Comparative table showing the results obtained when human sera were tested by IgA ELISA kits and by micro neutralization test to assess the contribution of the IgA antibodies on the neutralizing potency of the serum samples.

ID sample	Elisa Euroimmun	ELISA_VM_ IgG_S1	ELISA_VM_ IgG_RBD	ELISA_VM_ IgM_S1	ELISA_VM_ IgM_RBD	ELISA_VM_ IgA_RBD	MN Titres before IgA treatment	MN Titres after IgA treatment
158	Positive	Positive	Positive	Negative	Positive	Positive	20	20
159	Negative	Negative	Positive	Negative	Positive	Positive	20	20
160	Negative	Negative	Negative	Negative	Negative	Positive	20	20
161	Negative	Negative	Negative	Positive	Negative	Negative	n.a.	n.a.
162	Negative	Negative	Positive	Positive	Positive	Positive	n.a.	n.a.
163	Positive	Positive	Positive	Positive	Positive	Positive	40	40
164	Negative	Negative	Positive	Negative	Positive	Negative	n.a.	n.a.
165	Negative	Negative	Positive	Negative	Positive	Positive	80	40
166	Negative	Negative	Positive	Negative	Positive	Positive	80	40
167	Borderline	Negative	Positive	Positive	Positive	Negative	80	80
168	Negative	Positive	Positive	Negative	Positive	Positive	80	80
169	Negative	Negative	Positive	Negative	Positive	Positive	80	40
170	Positive	Positive	Positive	Positive	Positive	Positive	80	80
171	Negative	Negative	Positive	Negative	Positive	Positive	160	160
172	Positive	Positive	Positive	Negative	Positive	Positive	160	80
173	Positive	Positive	Positive	Positive	Positive	Negative	160	160
174	Positive	Negative	Positive	Positive	Positive	Positive	320	80
175–176	Positive	Positive	Positive	Positive	Positive	Positive	640	640
177	Positive	Positive	Positive	Negative	Positive	Positive	640	640
178–179	Positive	Positive	Positive	Positive	Positive	Positive	640	320
180–181	Positive	Positive	Positive	Positive	Positive	Positive	1280	640

A

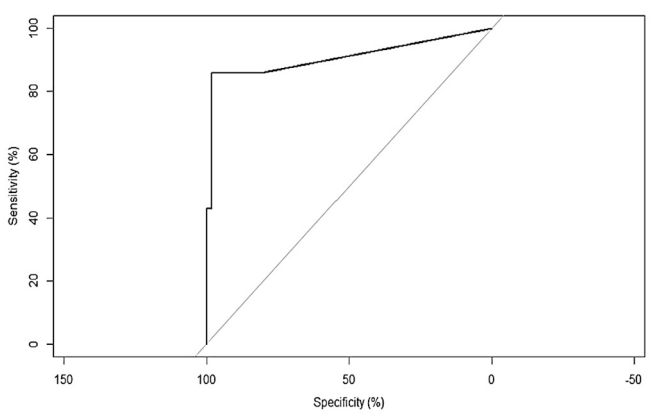

B

Cut-off	Sensitivity %	Specificity %
0.067	100	0
0.069	85.714	81.132
0.078	85.714	88.679
0.080	85.714	94.340
0.085	85.714	96.226
0.092	85.714	98.113
0.099	71.429	98.113
0.257	57.143	98.113
1.352	42.857	98.113
2.800	42.857	100
65.883	28.571	100
104921.201	14.286	100
Inf	0	100

C

	Predicted MNT		
True MNT	Positive	Negative	Total
Positive	6	1	7
Negative	1	52	53
Total	7	53	60

Fig. 2. A) Analysis of the ROC curve referred to the test set proved that the results of the EN model attained high accuracy in predicting the MNT values. Measurement of the area under the curve, AUC = 90.7%, supported this conclusion; B) Summary table of ROC analysis; C) Error matrix.

IgG1 and IgG3 was found in almost all samples, with the IgG3 subclass showing the highest percentage of detection. Low and very low reactivity was found for IgG4 and IgG3, respectively (Fig. 3).

3.5. *IgA antibodies increase the neutralization potency of the serum*

Due to the high correlation observed between the IgA ELISA and MN results we tried to assess the real contribution of the IgA antibodies on

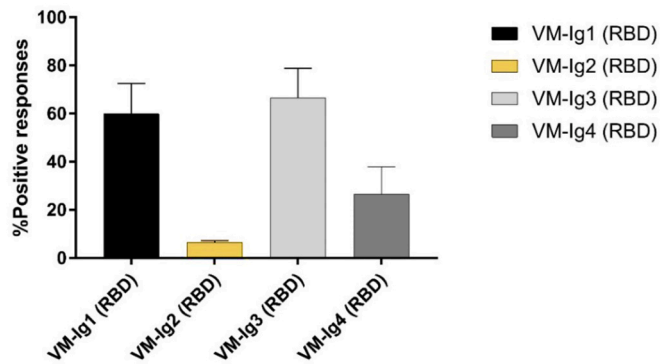

Fig. 3. Percentage of detection of IgG1, IgG2, IgG3 and IgG4 in all 14 human samples positive on MN assay. Each column represents the contribution, in terms of percentage, each IgG subclasses versus SARS- CoV- 2 RBD. Error bars showing the variance of sample proportion.

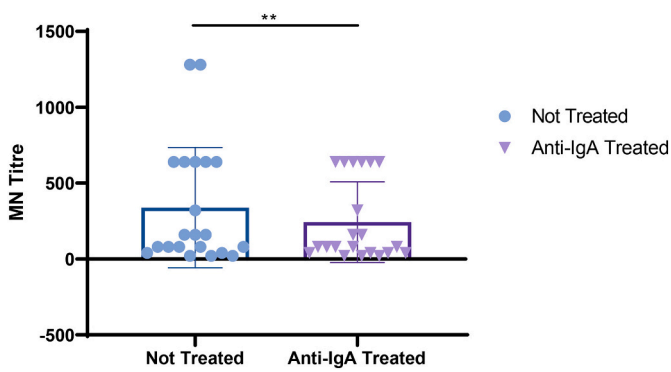

Fig. 4. Log transformed MNTs before and after the treatment with the goat anti-human IgA antibodies; *t*-Test shows a significant decrease in the MN titers for those samples with high neutralizing titers.

the neutralizing potency of the serum samples. As is possible to observe in Fig. 4 and Table 5, after the sample treatment we registered an evident decrease in the neutralizing titers. Interesting is the fact that the decrease is showed only in those sera that showed high starting neutralizing titers. Samples with medium/low MNTs did not show any decrease.

4. Discussion

Like most of the emerging infectious diseases that affect humans, this new HCoV also originated from animals (WHO, n.d.-b; Andersen et al., 2020). Owing to the rapid increase in some human practices, such as deforestation, urbanization and the husbandry of wild animal species, over the years the emergence of new pathogens has become an extremely serious problem. The rapid global spread of the novel SARS-CoV-2 is posing a serious health threat to the entire world. There is now an urgent need for well-standardized serological assays that can detect different classes of antibodies against the novel coronavirus, and which can be used alongside the classical diagnostic molecular methods such as RT-PCR. Indeed, due to the huge demand in the recent months, the availability of the reagents and equipment needed to promptly carry out analyses is still inadequate.

Moreover, if sample collection and storage are improperly conducted,molecular tests may yield false-negative results in subjects who carry the virus (Liu et al., 2020). Previous studies on SARS-CoV-1 have shown that virus-specific IgG and IgM levels can be valid surrogate for serological diagnosis (Guan et al., 2004; Hsueh et al., 2004). Indeed, the present study had two major goals: a) to standardize and make as reliable as possible ELISA tests in order to detect different classes of immunoglobulins, and b) to broaden the data-set of information on comparisons between the results of different serological tests, which could be precious for future evaluation of serological diagnoses and vaccine assessments (Madore et al., 2010). Specifically, in this study, ELISA results were always compared with those obtained by the functional assay (MN), which is commonly assumed as a benchmark and the gold standard.

Since its first isolation and characterization, this new HCoV strain has been classified, according to the WHO guidelines, as BSL3 pathogen. This has placed some limits on the implementation of neutralization tests, as relatively few laboratories have level-3 biocontainment facilities. The ELISAs are a good surrogate for the MN assay in terms of sensitivity, safety and throughput (Dessy et al., 2008; Gonda et al., 2012; Ivanov et al., 2019). However, it is very important to evaluate and estimate the best antigen/s to use in these platforms in order to obtain a reliable and similar response to that of the neutralization test, which indicates the functional response. This is why we compared all our results with those of the MNT. As in the case of influenza hemagglutinin (Clements et al., 1986), antibodies specific to the RBD domain of the S-protein seem to strongly contribute to viral neutralization. In this study, together with the IgG, IgM and IgA analyses, we also evaluated the responses of IgG subclasses in those subjects who showed both a high RBD ELISA signal and proven neutralization activity. Our results are in line with previous findings (Amanat et al., 2020) and confirm IgG1 and IgG3 as the subtypes with the strongest reactivity in all samples (Seow et al., 2020). Only in a small number of subjects did we find IgG2 and IgG4 responses. IgG1 and IgG3 are involved in critical immunologic functions, such as neutralization, opsonization, complement fixation and antibody-dependent cellular cytotoxicity (ADCC). On the other hand, IgG2 plays an important role in protecting against infection by encapsulated microorganisms (Ferrante et al., 1990); IgG4 is generally a minor component of the total immunoglobulin response and is induced in response to continuous antigenic stimulation (Aalberse et al., 1983).

Regarding the ELISA IgG, IgM and IgA, the main results can be summarized as follows: a) all the proposed statistical analyses indicated a close relationship between the results of MN and in-house RBD-based ELISAs, namely VM-IgG-RBD, VM-IgM-RBD and VM-IgA-RBD (results are in line with previous reports by Amanat and colleagues (Amanat et al., 2020; Okba et al., 2020)); b) the cross-validation technique applied to the EN model allowed us to obtain robust results.

In the out-of-sample data (i.e., the randomly chosen test-data) highly accurate, and, particularly, highly specific performance was observed; c) in large-scale screening operations, it is very important to have a highly specific test, as this guards against the risk of misclassification of true-negative samples with a wide margin of certainty. A highly specific test is particularly useful in order to confirm a diagnosis already made by means of other methods, and when a false-positive result would have a great impact. Indeed, a highly specific test is of most help to the clinician when it provides a positive result.

An overview of all the results yielded by ELISA and MN (data not shown), along with those obtained by treating the sample with anti-human IgA, reveals that the highest neutralization activity against SARS-CoV-2 is achieved when all three immunoglobulins, IgG, IgM and IgA are detected, as if to indicate the presence of a synergistic or additive effect between different classes of antibodies. This observation can be explained by the fact that the human population is completely naïve for SARS-CoV-2 and that IgG or IgM alone is not able to mount an ideal neutralizing immune response. Indeed, one of the most important features of adaptive immunity is the generation of immunological memory and the ability of the immune system to learn from its experiences of encounters with the same pathogen, thereby becoming more effective over time (Bonilla and Oettgen, 2010).

Interestingly, in nine samples, neither in-house nor commercial kits detected any IgG and IgM signal for the S1 protein, while a noticeable signal for RBD-specific IgG, IgM and IgA was detected.

As all nine samples displayed exactly same trend, it seems that these results could be due to the folding of the three-dimensional S1 protein structure after the production in HEK293 cells, which could have masked some epitopes recognized by the antibodies expressed in these nine subjects. By contrast, these epitopes may be well exposed in the RBD protein and can be bound by antibodies, which would explain the differences in signals.

To conclude, these results confirm what has already been reported (Robbiani et al., 2020), i.e. that the immune response to SARS-CoV-2 is very variable, but that antibodies targeting the RBD domain of Spike protein have an important role relatively to their neutralization activity. However, it is unclear whether neutralizing antibodies to S protein are the major contributor to a protective immune response as evidenced by a recent study (Hachim et al., 2020). So, the present study constitutes preliminary research into the development of an ELISA that can semi-quantify anti-SARS-CoV-2 human antibodies in a specific and repeatable way. The next step will be to completely validate these ELISAs according to the criteria established by the International Council for Harmonization of Technical Requirements for Pharmaceuticals for Human Use (Q 2 (R1), 2006), and to analyze the performance and specificity of these tests with a panel human serum samples that are highly positive towards different HCoVs.

Authors' contributions

LM performed the set-up experiments and standardized *in-house* ELISAs; LM, DM and IH performed all the ELISA experiments; PP evaluated the results and performed the statistical analyses; LB and IR handled the Vero E6 cells and prepared the plates for neutralization experiments; AM and EC performed the Micro-neutralization experiments; CMT and SM performed the Euroimmun ELISA assays at the University site and provided the human serum samples; AM and GL designed the experiments; AM, LM, EM (Eleonora Molesti) prepared the draft of the manuscript; EM supervised the study. All authors have approved the final version of the manuscript.

Acknowledgments

We thank the Laboratory of Molecular and Developmental Medicine of the University of Siena for providing the human serum samples. Furthermore, we thank Dr. Valentina Bollati from the University of Milan for providing the serum samples from COVID-19-positive patients. This publication was supported by the European Virus Archive Global (EVAg) project, which has received funding from the European Union's Horizon 2020 research and innovation program under grant agreement No 653316.

Declaration of Competing Interest

The authors declare that they have no conflict of interest.

References

Aalberse, R.C., Dieges, P.H., Knul-Bretlova, V., Vooren, P., Aalbers, M., van Leeuwen, J., Jun. 1983. IgG4 as a blocking antibody. Clin. Rev. Allergy 1 (2), 289–302. https://doi.org/10.1007/BF02991163.

Amanat, F., et al., May 2020. A serological assay to detect SARS-CoV-2 seroconversion in humans. Nat. Med. 1–4. https://doi.org/10.1038/s41591-020-0913-5.

Andersen, K.G., Rambaut, A., Lipkin, W.I., Holmes, E.C., Garry, R.F., Apr. 2020. The proximal origin of SARS-CoV-2. Nat. Med. 26 (4) https://doi.org/10.1038/s41591-020-0820-9. Art. no. 4.

Andreano, E., et al., May 2020. Identification of neutralizing human monoclonal antibodies from Italian Covid-19 convalescent patients. Immunology. https://doi.org/10.1101/2020.05.05.078154 preprint.

Bao, L., et al., Mar. 2020. Lack of Reinfection in Rhesus Macaques Infected with SARS-CoV-2. Microbiology. https://doi.org/10.1101/2020.03.13.990226 preprint.

Berry, J.D., et al., 2010. Neutralizing epitopes of the SARS-CoV S-protein cluster independent of repertoire, antigen structure or mAb technology. mAbs 2 (1), 53–66.

Bonilla, F.A., Oettgen, H.C., Feb. 2010. Adaptive immunity. J. Allergy Clin. Immunol. 125 (2), S33–S40. https://doi.org/10.1016/j.jaci.2009.09.017.

Chan, J.F.-W., et al., 2020. A familial cluster of pneumonia associated with the 2019 novel coronavirus indicating person-to-person transmission: a study of a family cluster. Lancet Lond. Engl. 395 (10223), 514–523. https://doi.org/10.1016/S0140-6736(20)30154-9.

Clements, M.L., Betts, R.F., Tierney, E.L., Murphy, B.R., Jul. 1986. Serum and nasal wash antibodies associated with resistance to experimental challenge with influenza A wild-type virus. J. Clin. Microbiol. 24 (1), 157–160.

Corman, V.M., Lienau, J., Witzenrath, M., 2019. Coronaviren als Ursache respiratorischer Infektionen. Internist 60 (11), 1136–1145. https://doi.org/10.1007/s00108-019-00671-5.

Dessy, F.J., et al., Nov. 2008. Correlation between direct ELISA, single epitope-based inhibition ELISA and Pseudovirion-based neutralization assay for measuring anti-HPV-16 and anti-HPV-18 antibody response after vaccination with the AS04-adjuvanted HPV-16/18 cervical cancer vaccine. Hum. Vaccine 4 (6), 425–434. https://doi.org/10.4161/hv.4.6.6912.

Ferrante, A., Beard, L.J., Feldman, R.G., Aug. 1990. IgG subclass distribution of antibodies to bacterial and viral antigens. Pediatr. Infect. Dis. J. 9 (8 Suppl), S16–S24.

Frasca, D., Diaz, A., Romero, M., Mendez, N.V., Landin, A.M., Blomberg, B.B., Apr. 2013. Effects of age on H1N1-specific serum IgG1 and IgG3 levels evaluated during the 2011–2012 influenza vaccine season. Immun. Ageing A 10 (1), 14. https://doi.org/10.1186/1742-4933-10-14.

Gonda, M.G., Fang, X., Perry, G.A., Maltecca, C., Oct. 2012. Measuring bovine viral diarrhea virus vaccine response: using a commercially available ELISA as a surrogate for serum neutralization assays. Vaccine 30 (46), 6559–6563. https://doi.org/10.1016/j.vaccine.2012.08.047.

Gorbalenya, A.E., et al., Apr. 2020. The species Severe acute respiratory syndrome-related coronavirus : classifying 2019-nCoV and naming it SARS-CoV-2. Nat. Microbiol. 5 (4) https://doi.org/10.1038/s41564-020-0695-z (Art. no. 4).

Guan, M., Chen, H.Y., Foo, S.Y., Tan, Y.-J., Goh, P.-Y., Wee, S.H., Mar. 2004. Recombinant protein-based enzyme-linked immunosorbent assay and Immunochromatographic tests for detection of immunoglobulin G antibodies to Severe Acute Respiratory Syndrome (SARS) coronavirus in SARS patients. Clin. Diagn. Lab. Immunol. 11 (2), 287–291. https://doi.org/10.1128/CDLI.11.2.287-291.2004.

Hachim, A., et al., Oct. 2020. ORF8 and ORF3b antibodies are accurate serological markers of early and late SARS-CoV-2 infection. Nat. Immunol. 21 (10), 1293–1301. https://doi.org/10.1038/s41590-020-0773-7.

Hsueh, P.-R., et al., Sep. 2004. SARS antibody test for serosurveillance. Emerg. Infect. Dis. 10 (9), 1558–1562. https://doi.org/10.3201/eid1009.040101.

Ivanov, A.P., Klebleyeva, T.D., Malyshkina, L.P., Ivanova, O.E., 2019. Poliovirus-binding inhibition ELISA based on specific chicken egg yolk antibodies as an alternative to the neutralization test. J. Virol. Methods 266, 7–10. https://doi.org/10.1016/j.jviromet.2019.01.007.

Kundi, M., Apr. 1999. One-hit models for virus inactivation studies. Antivir. Res. 41 (3), 145–152. https://doi.org/10.1016/s0166-3542(99)00008-x.

Liu, W., et al., 2020. Evaluation of nucleocapsid and spike protein-based enzyme-linked immunosorbent assays for Detecting antibodies against SARS-CoV-2. J. Clin. Microbiol. 58 (6) https://doi.org/10.1128/JCM.00461-20.

Madore, D.V., Meade, B.D., Rubin, F., Deal, C., Lynn, F., Jun. 2010. Utilization of serologic assays to support efficacy of vaccines in nonclinical and clinical trials: meeting at the crossroads. Vaccine 28 (29), 4539–4547. https://doi.org/10.1016/j.vaccine.2010.04.094.

Manenti, A., et al., 2017. Comparative analysis of influenza A(H3N2) virus hemagglutinin specific IgG subclass and IgA responses in children and adults after influenza vaccination. Vaccine 35 (1), 191–198. https://doi.org/10.1016/j.vaccine.2016.10.024.

Manenti, A., et al., May 2020. Evaluation of SARS-CoV-2 neutralizing antibodies using a CPE-based colorimetric live virus micro-neutralization assay in human serum samples. J. Med. Virol. https://doi.org/10.1002/jmv.25986.

Murin, C.D., Wilson, I.A., Ward, A.B., 2019. Antibody responses to viral infections: a structural perspective across three different enveloped viruses. Nat. Microbiol. 4 (5), 734–747. https://doi.org/10.1038/s41564-019-0392-y.

Okba, N.M.A., et al., Jul. 2020. Severe acute respiratory syndrome coronavirus 2-specific antibody responses in coronavirus disease patients. Emerg. Infect. Dis. 26 (7), 1478–1488. https://doi.org/10.3201/eid2607.200841.

Ou, X., et al., 2016. Identification of the Fusion Peptide-Containing Region in Betacoronavirus Spike Glycoproteins. J. Virol. 90 (12), 5586–5600. https://doi.org/10.1128/JVI.00015-16.

Q 2 (R1), 2006. Validation of Analytical Procedures: Text and Methodology, p. 15.

Robbiani, D.F., et al., Jun. 2020. Convergent antibody responses to SARS-CoV-2 in convalescent individuals. Nature. https://doi.org/10.1038/s41586-020-2456-9.

Schroeder, H.W., Cavacini, L., Feb. 2010. Structure and function of immunoglobulins. J. Allergy Clin. Immunol. 125 (2 Suppl 2), S41–S52. https://doi.org/10.1016/j.jaci.2009.09.046.

Seow, J., et al., Jul. 2020. Longitudinal evaluation and decline of antibody responses in SARS-CoV-2 infection. Infectious Diseases (except HIV/AIDS). https://doi.org/10.1101/2020.07.09.20148429 preprint.

Tay, M.Z., Poh, C.M., Rénia, L., MacAry, P.A., Ng, L.F.P., Jun. 2020. The trinity of COVID-19: immunity, inflammation and intervention. Nat. Rev. Immunol. 20 (6) https://doi.org/10.1038/s41577-020-0311-8. Art. no. 6.

WHO, 2020. Coronavirus disease 2019 (COVID19) Situation Report 23. In: Coronavirus disease 2019 (COVID-19) Situation Report - 23. https://www.who.int/docs/default-source/coronaviruse/situation-reports/20200212-sitrep-23-ncov.pdf?sfvrsn=41e9fb78_4 (accessed 10.07.20).

WHO. Coronavirus disease COVID-19 Situation Reports - Weekly Updates. https://www.who.int/emergencies/diseases/novel-coronavirus-2019/situation-reports (accessed 23.09.20).

WHO, Manual for the laboratory diagnosis and virological surveillance of influenza', WHO. https://www.who.int/influenza/gisrs_laboratory/manual_diagnosis_surveillance_influenza/en/ (accessed 10.07.20).

de Wit, E., van Doremalen, N., Falzarano, D., Munster, V.J., 2016. SARS and MERS: recent insights into emerging coronaviruses. Nat. Rev. Microbiol. 14 (8), 523–534. https://doi.org/10.1038/nrmicro.2016.81.

Wrapp, D., et al., Mar. 2020. Cryo-EM structure of the 2019-nCoV spike in the prefusion conformation. Science 367 (6483), 1260–1263. https://doi.org/10.1126/science.abb2507.

Zaki, A.M., van Boheemen, S., Bestebroer, T.M., Osterhaus, A.D.M.E., Fouchier, R.A.M., Nov. 2012. Isolation of a novel coronavirus from a man with pneumonia in Saudi Arabia. N. Engl. J. Med. 367 (19), 1814–1820. https://doi.org/10.1056/NEJMoa1211721.

Zou, H., Hastie, T., Apr. 2005. Regularization and variable selection via the elastic net. J. R. Stat. Soc. Ser. B Stat Methodol. 67 (2), 301–320. https://doi.org/10.1111/j.1467-9868.2005.00503.x.

Zou, L., et al., Mar. 2020. SARS-CoV-2 viral load in upper respiratory specimens of infected patients. N. Engl. J. Med. 382 (12), 1177–1179. https://doi.org/10.1056/NEJMc2001737.